Evolution of Radiation Dose from Cardiac CT

2

Manoj Mannil and Hatem Alkadhi

Cardiac imaging with computed tomography (CT) remains a challenging task requiring both a high spatial resolution for imaging of the relatively small coronary arteries and a high temporal resolution for providing motion-free images of the heart. In parallel to technological advances, tireless efforts to simultaneously reduce radiation dosages were implemented. As in any given body region, these measures are based on the following two principles: restricting the total number of cardiac CT examinations by close adherence to guidelines and recommendations and reducing the radiation of each individual CT study according to the "as low as reasonably achievable" (ALARA) principle while maintaining a diagnostic image quality [1]. This chapter focuses on the latter.

Introduction of various CT protocol developments and software modifications such as tube current modulation, automatic tube potential selection, electrocardiography (ECG) pulsing, and iterative reconstruction enabled the decrease of ionizing radiation dose in one order of magnitude over the last two decades [2] (Table 2.1).

ECG Gating

Cardiac CT imaging must be performed with ECG gating, in order to freeze all images in defined time points of the cardiac cycle. At normal heart rates, least cardiac motion occurs during diastole, when the ventricles are filling. Three

Table 2.1 Abbreviations and terms for cardiac CT imaging

Abbreviations and terms	Description
AEC	Automatic exposure control mechanism for dose optimization in CT, which adapts tube current according to the part of the body being scanned to obtain the desired image quality
CTDI	Computed tomography dose index: Radiation dose of a single slice from the primary beam and scatter from surrounding slices, in milligrays [mGy]
CTDIvol	Computed tomography dose index volume: A measure describing the radiation dose factoring in pitch, which represents the average radiation dose in three dimensions and is typically reported in milligrays [mGy]
DLP	Dose length product reflects the total energy absorbed attributable to a complete CT scan acquisition and is determined by multiplying the CTDIvol by the scan length [mGy*cm]
ECG pulsing	Modulation of the tube current according to the electrocardiogram (ECG). Peak tube output during a selected pulsing window and reduction of the tube output to approximately 25% during remaining parts of the cardiac cycle
IR	Iterative reconstruction: Image reconstruction algorithm that localizes and selectively removes image noise. Repetitive comparison of reconstructed images with a computed expected data set
Pitch	Defined as table distance traveled in one 360° gantry rotation divided by beam collimation in single-slice CT or total thickness of all simultaneously acquired slices in multislice CT
Reconstructed slice thickness	Width of a single slice in the reconstructed image [mm]. The greater the slice thickness, the more X-ray photons are present in the raw data for reconstructing the image, with an effect on image noise similar to that of increasing the tube current
TCM	Tube current modulation automatically adapts the mAs delivered during the CT scan based on patient thickness determined from the topogram

M. Mannil (✉) · H. Alkadhi
Institute of Diagnostic and Interventional Radiology, University Hospital Zurich, Zurich, Switzerland
e-mail: manoj.mannil@usz.ch

U. J. Schoepf (ed.), *CT of the Heart*, Contemporary Medical Imaging, https://doi.org/10.1007/978-1-60327-237-7_2

approaches for ECG gating are currently used: (1) retrospective ECG gating with spiral data acquisition, (2) prospective ECG gating with a sequential (or "step-and-shoot") data acquisition, and (3) prospective ECG gating with spiral data acquisition and high pitch.

Retrospective ECG Gating

In retrospective ECG-gating techniques, partially overlapping multi-detector CT projections are continuously acquired in the spiral mode, and the ECG signal is simultaneously recorded. Software algorithms are then used to sort the data from different phases of the cardiac cycle by progressively shifting the temporal window of acquired helical projection data relative to the R wave (Fig. 2.1). Every position of the heart is covered by a detector row at every point of the cardiac cycle. Therefore, the scanner table continuously moves but advances not more than the total width of the active detectors for each heartbeat [3]. For a gapless volume coverage of the heart in each cardiac phase, a low table feed (pitch <1) is required, which has to be adapted to the heart rate of the patient: the higher the heart rate, the faster the table can move. Using a 4-cm detector enables covering the entire heart volume in 3–4 heartbeats [4]. Due to the low pitch of this imaging technique, the same anatomic area is repeatedly exposed to ionizing radiation during consecutive rotations of the gantry, which results in a relatively higher radiation dose as compared to the other ECG-gating techniques described below. Radiation dose values of up to 21 mSv have been initially reported for this technique with 64-slice CT.

The use of ECG pulsing allows for modulation of the tube current according to the ECG. The peak tube output is generated during a selected pulsing window, usually during diastole. During the remaining parts of the cardiac cycle, the tube output is reduced to approximately 25%. Most scanners allow to adjust the ECG-pulsing window width according to the heart rate, in order to be as narrow as possible for maximal radiation exposure reduction while being as wide as reasonable to obtain diagnostic image quality at the same time [5]. Modern ECG-pulsing algorithms are able to automatically detect arrhythmia and switch off ECG pulsing during ectopic heartbeats.

When combining retrospective ECG gating with optimized tube voltage and tube current in combination with modern iterative reconstruction algorithms, radiation doses can be as low as 4–6 mSv per cardiac CT examination with this technique.

Prospective ECG Gating in the Sequential Mode

Prospective ECG triggering uses the ECG signal to limit scanning to time points defined prior to the data acquisition, usually during diastole. Projection data are acquired during more than half a gantry rotation. The total number of slices produced per heartbeat during this half rotation of the gantry is proportional to the number of rows of active detectors. As

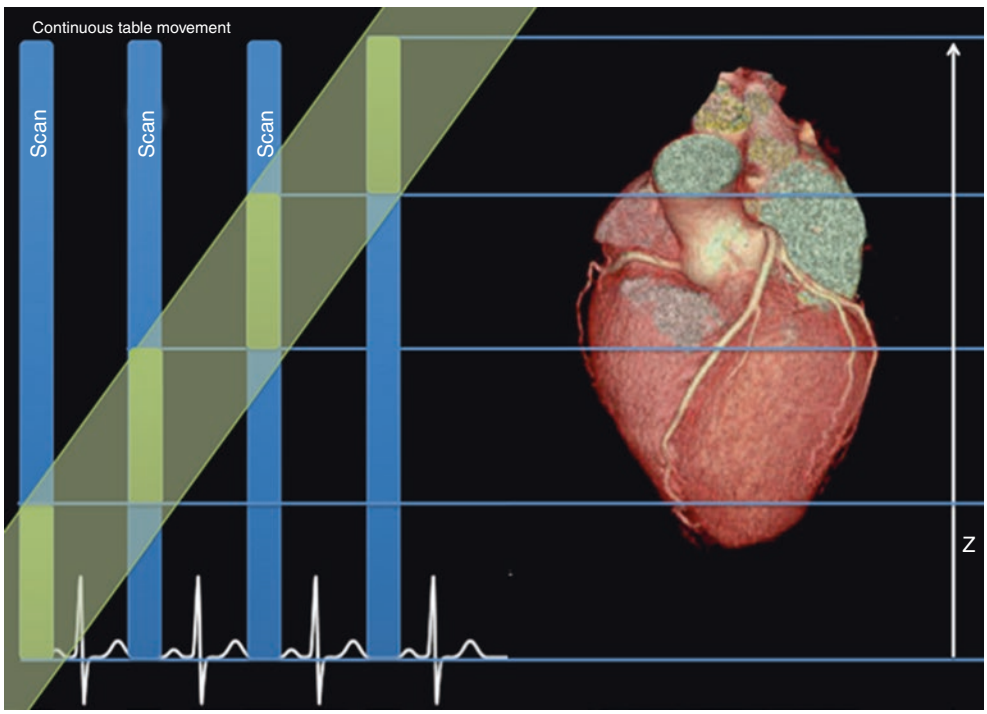

Fig. 2.1 Retrospective ECG-gated cardiac CT in the spiral mode with continuous table movement. The ECG of the patient is schematically shown at the bottom. Data can be retrospectively reconstructed at each after data acquisition at each time point of the cardiac cycle. (Modified from Flohr et al. [4], with permission)

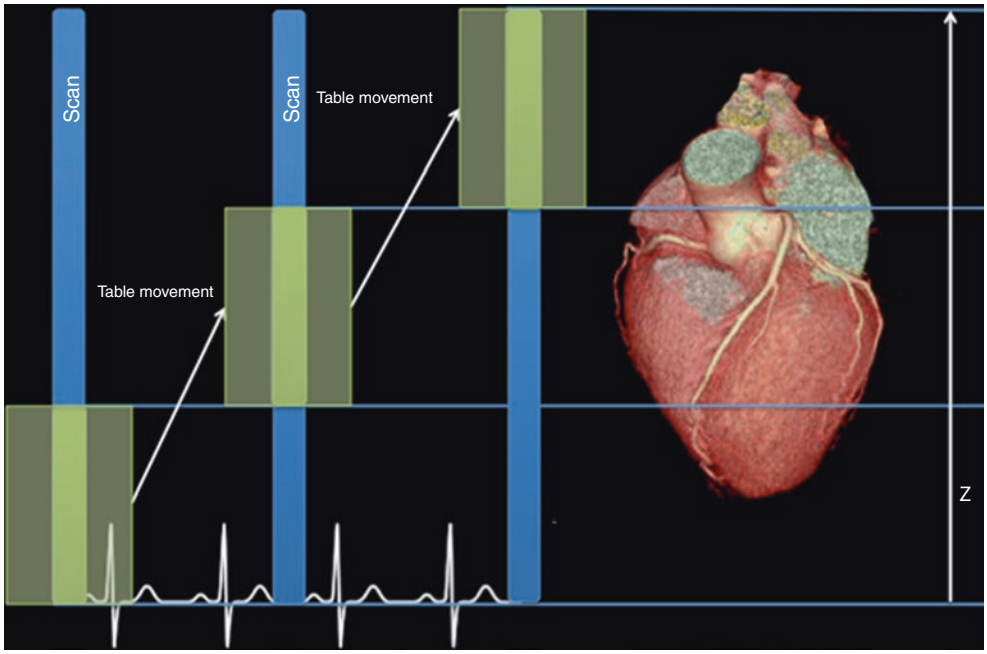

Fig. 2.2 Principle of prospective ECG-gated sequential (or "step-and-shoot") scanning. The ECG of the patient is schematically shown at the bottom. The blue lines indicate the z-positions of the individual detector rows of a multirow detector relative to the patient. Axial (sequential) scan data are acquired with a user-selectable temporal distance to the preceding R wave. After each axial scan, the table moves to the next z-position. Scan data are typically acquired at every second heartbeat. (Modified from Flohr et al. [4], with permission)

axial (rather than helical) scanning is used, the table is not moving during but only in-between data acquisition. The table has to move by the total collimation width after each acquisition (sequential or "step-and-shoot" mode) (Fig. 2.2). About 12 cm of scanning in the z-axis is required to cover most adult hearts; the total number of heartbeats and number of image stacks for a cardiac CT study depend on the width of the detector. However, as the scan is sequentially obtained, there is minimal flexibility in retrospectively choosing different phases of the cardiac cycle for image reconstruction. This minimal flexibility can be circumvented by using the technique of "padding." Padding allows for acquisition of images in additional cardiac phases by extending the mandatory minimum acquisition time. There is a trade-off between acquisition flexibility and radiation dose. Extensive use of padding is associated with a greater radiation dose. For instance, a 100 millisecond increase in padding results in a 45% increase in radiation dose [6]. A recent meta-analysis showed that prospective ECG gating is associated with an average radiation dose of 2.7 mSv [7]. Currently, prospective ECG gating is the most widely used technique for data acquisition in cardiac CT [2, 8].

Prospective ECG Gating with Spiral Acquisition and High Pitch

Since the commercial launch of dual-source CT technology in 2005, further reduction of ionizing radiation was achieved through use of prospective ECG gating with high pitch. In this mode, data is acquired in a spiral fashion, while the table runs with a high pitch (e.g., 3.2 with third-generation dual-source CT, equivalent to a table feed of 737 cm/s).

Using this technique yields a "snapshot" scan of the entire heart within one cardiac cycle, usually during diastole. While pitch in a single-source CT is limited to values of approximately 1.5 to ensure gapless volume coverage along the z-axis, a dual-source CT system contains a second X-ray tube at 90° offset, which acquires scan data at the same angular position at a quarter rotation later. This facilitates a maximum pitch of 3.2–3.4, depending on the scanner generation, within a limited scan field of view (FOV) covered by both detectors (Fig. 2.3). A quarter rotation of data per measurement system is used for image reconstruction, and each individual axial image has a temporal resolution of a quarter of the gantry rotation time. The ECG is used to prospectively trigger the start of table motion and the start of the high-pitch spiral. A requirement for usage of this technique is generally a stable sinus rhythm with heart rates ≤60 bpm with second-generation dual-source CT and ≤70 bpm with third-generation dual-source CT (Fig. 2.4).

The effective radiation dose of a prospectively ECG-gated high-pitch cardiac CT can be well below 1 mSv [9, 10]. In contrast to prospective ECG gating, where additional X-ray exposure along the entire width of the detector is generated at every slice, the high-pitch mode generates superfluous X-rays exposing the entire width of the detector only at the beginning and at the end of the spiral path. This explains the further reduction of radiation exposure when using this mode [1].

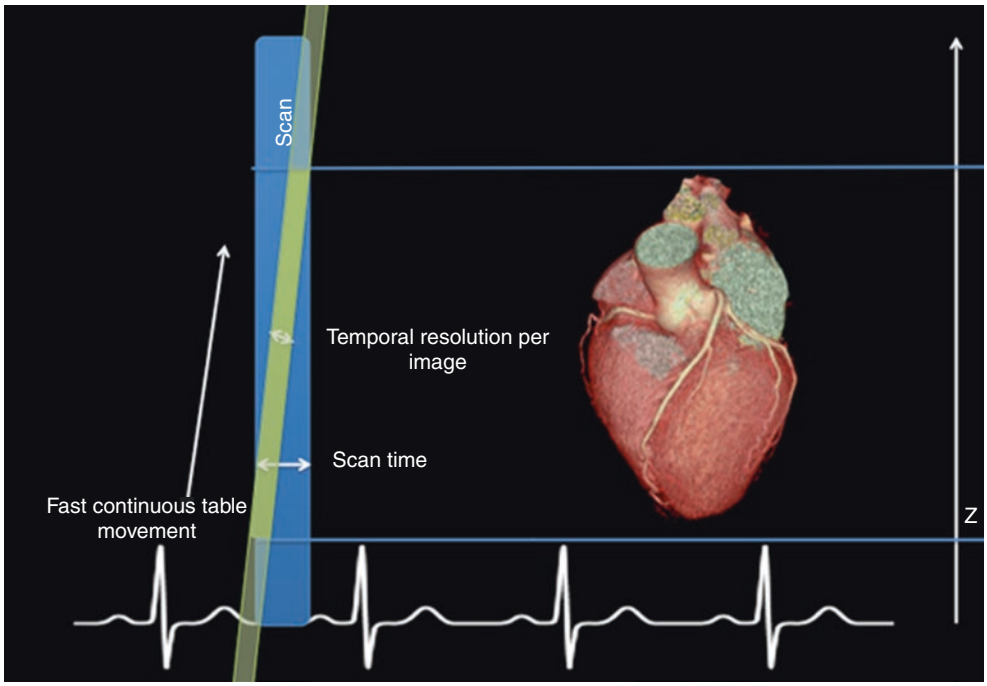

Fig. 2.3 ECG-gated high-pitch mode. The ECG of the patient is schematically shown at the bottom. The table is moved at very high speed, sufficient to cover the entire heart volume within a single diastole. At each z-position, only the minimum amount of scan data necessary for image reconstruction is acquired. The temporal resolution per image is therefore close to a quarter of the gantry rotation time; and there is a slight phase shift of the reconstructed images along the z-axis. (Modified from Flohr et al. [4], with permission)

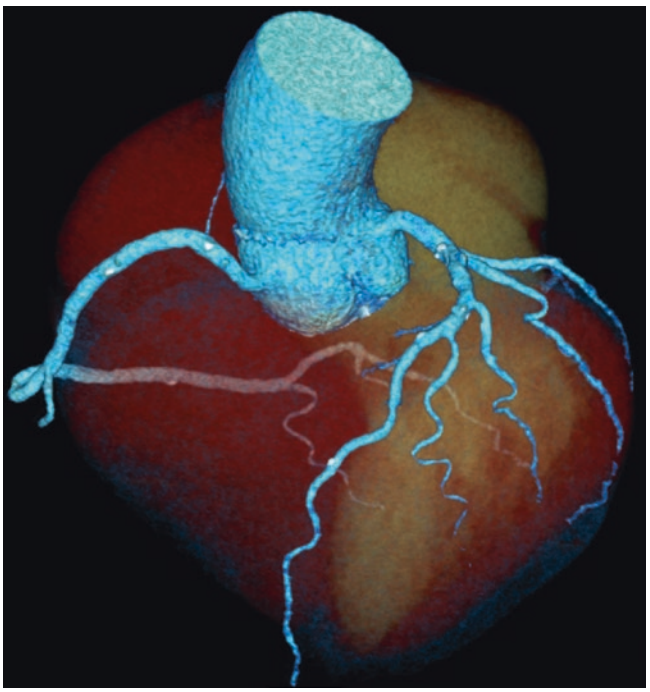

Fig. 2.4 3D image of the coronary artery tree with volume rendering of image data acquired with the high-pitch mode on a third-generation dual-source CT scanner. Estimated effective radiation dose was 0.4 mSv

Tube Current Modulation and Tube Voltage Adaptation

Both tube current modulation and tube voltage adaptation can be used for all scan protocols described above. Tube current modulation is defined as automatic adjustment of the tube current to account for differences in body shape and attenuation depending on the body region scanned. Lowering and optimizing the tube voltage represent another important approach for dose reduction, as radiation dose varies with the square of the tube voltage. Initial investigations with 16-/64-slice CT systems comparing 120- and 100-kV tube voltage CT protocols have shown that decreased tube voltages reduce overall radiation dose at the expense of increased image noise. The signal-to-noise (SNR) and contrast-to-noise ratios (CNR), however, remain unaffected, as decreased tube voltages approach the k-edge of iodine (33.2 keV), which results in higher attenuation of iodinated contrast. With an increase in both parameters, signal/contrast and noise, the overall ratios for SNR and CNR remain unaffected [11–13]. Recently, automatic tube potential selection algorithms became available which automatically lower the tube potential according to patient size, diagnostic task, and scanner tube current limits. This measurement is reported to yield a dose reduction between 20% and 50% in nonobese patient populations. For larger patients, however, image quality may deteriorate beyond diagnostic quality [14].

Iterative Reconstruction (IR)

Iterative reconstruction (IR) is a technique that incorporates statistical modeling in image reconstruction with the main aim to reduce image noise. This technique can be also used for reducing the radiation dose (usually through reduced tube current) while maintaining the image quality of the examination [1, 10]. Similar to the options tube current modulation and tube voltage adaptation, IR can be applied for all scan protocols described above.

Filtered Back Projection (FBP)

Until recently, CT images were almost exclusively reconstructed with filtered back projection (FBP), largely due to the fact that FBP generates diagnostic images at a low level of computational complexity. In FBP the X-ray beam assumes a pencil shape, and the X-ray source is aligned in a parallel fashion to a linear X-ray detector array. For image generation, the X-ray source is rotated over a certain angle, allowing for intensities to be measured at the detector. These intensities are described as an integral function for a specific angle and the shift in the position of the X-ray tube. After this, the reconstruction process involves solving an integral equation by inversion or so-called back projection. Despite its ability to rapidly reconstruct images, FBP has various limitations, in particular increased image noise, which is most prominent in low tube current imaging, poor contrast resolution, and streak artifacts. This is primarily due to the inherent failure of the FBP algorithm to account for image noise that results from Poisson statistical variations in the number of photons across the imaging plane, leading to an inverse relationship between radiation dose and image noise. Until the recent introduction of IR, lowering image noise could only be achieved at the expense of increased radiation dose. Attempts at so-called image-based denoising through smoothing algorithms and filters (convolution kernels) allow for noise reduction but result in compromised spatial resolution and image fidelity [15].

Iterative Reconstruction (IR)

In principle, IR techniques attempt to localize and selectively remove image noise by frequent comparison with a canvas. This is achieved through a process of modeling the imaging acquisition process, including fluctuations in photon statistics, the optics system, and various aspects of X-ray interactions to generate an expected data set, which is then compared to the actually acquired data set. The differences between these two are used to identify and remove noise, and the process is repeated multiple times until the updated data converges with or approximates the expected data to maximize image optimization.

Initially, *statistical* IR was introduced in CT imaging. It deals with noise due to fluctuations in photon statistics by assigning a relatively higher weighting to data with low statistical uncertainty (low noise) and lesser weighting to data with high statistical uncertainty (high noise). It operates in either the "raw data domain" with subsequent reconstruction using the "noise-reduced" data or in the "image domain" after IR. More recently, IR algorithms that model for the physical three-dimensional nature of the system optics (geometric modeling of the focal point of the X-ray tube and pixel detector) and the interaction of photons in the transmission between the X-ray tube, isocenter, and detector (physical modeling) have been developed and are collectively referred to as model-based IR [15]. Current IR algorithms typically combine statistical modeling with model-based IR. In hybrid IR algorithms, the imaging data can be blended with traditional FBP at certain thresholds. The iteratively reconstructed CT images are generally less noisy and possess an improved image resolution and edge detection compared to images acquired with FBP (Fig. 2.5).

Due to this circumstance, diagnostic images can be achieved even at lower tube currents when using IR instead of FBP, and radiation exposure can be significantly decreased. Many studies have evaluated noise and dose reduction with IR algorithms across multiple vendors (Table 2.2). In summary they demonstrate either (1) improved noise properties with IR compared to FBP when images from the same patients are reconstructed using both algorithms (intraindividual analysis) or (2) preserved subjective image quality and quantitative noise properties among patients undergoing IR image reconstruction with low-radiation dose techniques (reduced tube current and/or potential) compared to FBP algorithms with standard dose techniques (interindividual analysis). For instance, performing prospectively ECG-gated high-pitch coronary angiography with third-generation dual-source CT and using advanced modeled IT at a 70 kVp tube voltage result in a reduced image noise and improved overall image quality compared to standard FBP reconstructions at an average effective dose of only 0.3 mSv [15, 16].

Limiting the Scan Length

Limiting the scan length, or z-axis coverage, to exactly encompass the heart and coronary arteries represents another important factor for reducing the radiation dose cardiac CT. Traditionally, each cardiac CT examination starts with acquisition of a scout view for planning the scan length of the examination. It is a common practice to obtain an unenhanced low-dose calcium scoring scan, whose scan length is usually planned on the scout view. Then, contrast-enhanced CT coronary angiography is performed for diagnosing or excluding coronary artery stenoses. Due to the limited anatomic information provided by the scout view, the exact cranio-caudal extent of the coronary arteries cannot be discerned on a scout view. Therefore, the region of the carina is frequently used as the upper border and the cardiac apex as the lower border of the scan length of CT coronary angiography.

Alternatively, scan length can be determined by using the axial images from calcium scoring for identifying the table position at the origin of the left main artery and that

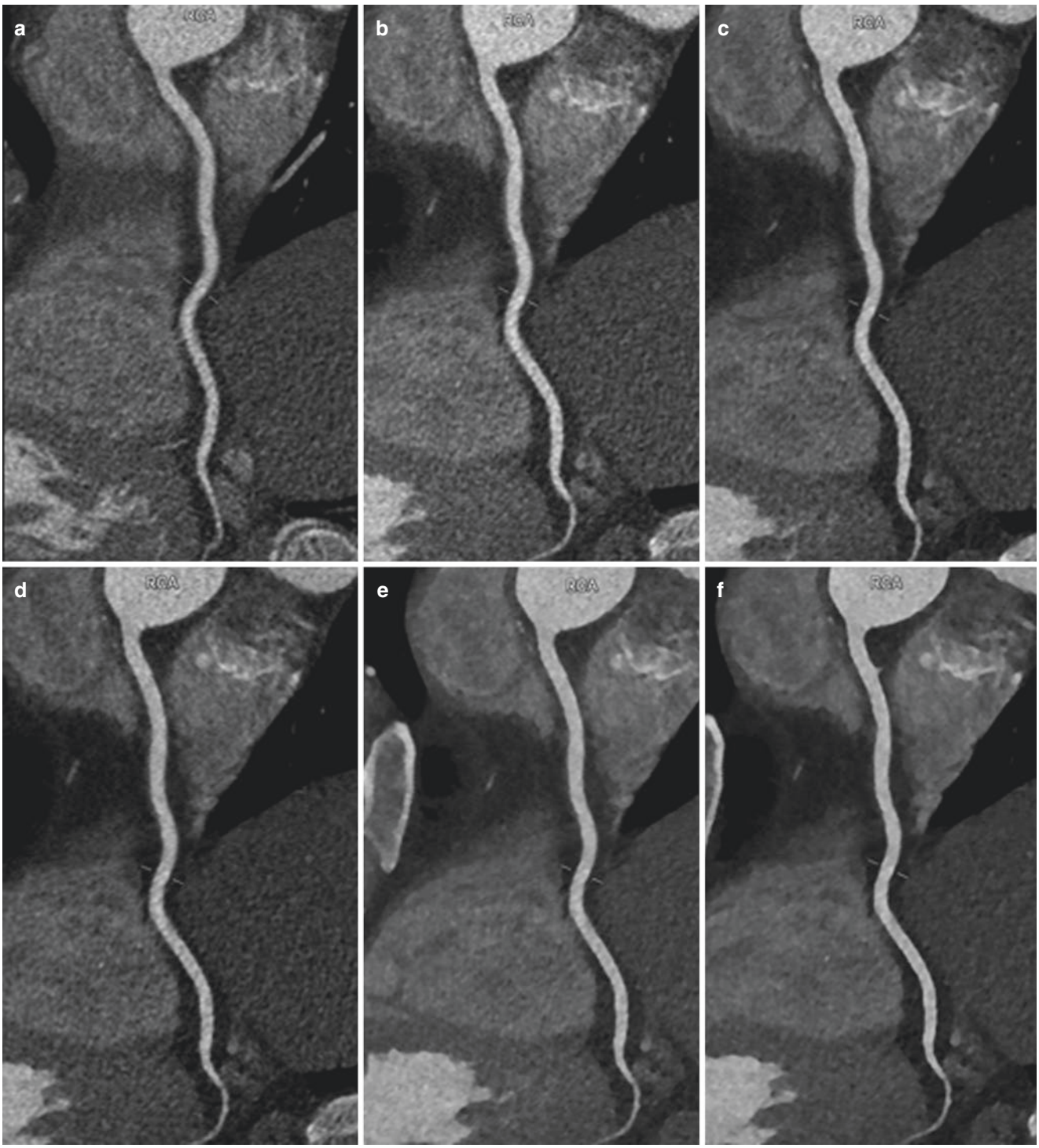

Fig. 2.5 Multiplanar reformations of the right coronary artery using (**a**) filtered back projection (FBP), (**b**) advanced modeled iterative reconstruction (ADMIRE) strength level 1, (**c**) ADMIRE strength level 2, (**d**) ADMIRE strength level 3, (**e**) ADMIRE strength level 4, (**f**) ADMIRE strength level 5. Note the continuous decrease of image noise and the improved vessel sharpness from FBP to ADMIRE images

Table 2.2 Iterative reconstruction algorithms by vendor

Iterative reconstruction technique	Vendor	Type
Adaptive statistical iterative reconstruction (ASIR)	General Electric (GE) Healthcare	Hybrid
Model-based iterative reconstruction (MBIR-Veo)	General Electric (GE) Healthcare	Model-based
Adaptive statistical iterative reconstruction (ASIR-V)	General Electric (GE) Healthcare	Hybrid
iDose	Philips Healthcare	Hybrid
Iterative model reconstruction (IMR)	Philips Healthcare	Model-based
Iterative reconstruction in image space (IRIS)	Siemens Healthcare	Hybrid
Sinogram-affirmed iterative reconstruction (SAFIRE)	Siemens Healthcare	Hybrid
Advanced modeled iterative reconstruction (ADMIRE)	Siemens Healthcare	Hybrid
Adaptive iterative dose reduction (AIDR)	Toshiba	Hybrid
Adaptive iterative dose reduction 3D (AIDR 3D)	Toshiba	Hybrid

of the cardiac apex. The scan length for CT coronary angiography can be then planned by adding around 1 cm to the cranial and around 1 cm to the lower border to account for possible changes in inspiration depth between calcium scoring and CT coronary angiography. Using this approach might lead to another reduction of radiation exposure of around 16% [17].

Clinical Relevance of Dose Reduction and Cancer Risk

Raised awareness of medical practitioners and stringent application of the aforementioned dose reduction techniques have been proven to be effective. Cardiac CT is well established for certain indications, e.g., for ruling out obstructive coronary artery disease at a low-to-intermediate pretest probability [18]. For determining whether all efforts in minimizing ionizing radiation are relevant requires comparison of the clinical benefit of the CT examination with the potential and theoretical cancerogenic risk of the procedure.

Reports on cancer risk in medical imaging are mainly derived from extrapolations of risk estimates to low levels of radiation and multiplications with a large number of exposed individuals. However, the data extrapolation is not reliable below an exposure of 100 mSv. Therefore, various different hypotheses about extrapolation of radiation risk to lower radiation doses were formulated, including a linear no-threshold model which indicates that each level of radiation is associated with a risk to the patient and that there is no lower threshold for this risk. Still, the American Association of Physicists in Medicine considers risks of medical imaging at effective doses <50 mSv for single procedures or <100 mSv for multiple procedures over short-time periods as too low to be epidemiologically detectable. While there is no evidence between radiation from medical imaging and cancer induction in a general adult population, it is in the best interests of the patients to keep the ionizing radiation exposure ALARA, without loss of diagnostic information.

Summary

Recent technological advances in cardiac CT imaging, ranging from automated exposure control, tube voltage optimization, scan length adjustments, evolution of ECG-gating techniques, and iterative reconstruction post-processing, have reduced radiation doses in one order of magnitude over the last decade. Continuous efforts in the optimal selection of each of the techniques help in keeping the radiation exposure to each individual adult patient so low that the assumed theoretical radiation risk from cardiac CT can be neglected.

References

1. Alkadhi H, Leschka S. Radiation dose of cardiac computed tomography - what has been achieved and what needs to be done. Eur Radiol. 2011;21(3):505–9.
2. den Harder AM, Willemink MJ, de Jong PA, Schilham AM, Rajiah P, Takx RA, et al. New horizons in cardiac CT. Clin Radiol. 2016;71(8):758–67.
3. Desjardins B, Kazerooni EA. ECG-gated cardiac CT. AJR Am J Roentgenol. 2004;182(4):993–1010.
4. Flohr TG, De Cecco CN, Schmidt B, Wang R, Schoepf UJ, Meinel FG. Computed tomographic assessment of coronary artery disease: state-of-the-art imaging techniques. Radiol Clin North Am. 2015;53(2):271–85.
5. Leschka S, Scheffel H, Desbiolles L, Plass A, Gaemperli O, Valenta I, et al. Image quality and reconstruction intervals of dual-source CT coronary angiography: recommendations for ECG-pulsing windowing. Investig Radiol. 2007;42(8):543–9.
6. Labounty TM, Leipsic J, Min JK, Heilbron B, Mancini GB, Lin FY, et al. Effect of padding duration on radiation dose and image interpretation in prospectively ECG-triggered coronary CT angiography. AJR Am J Roentgenol. 2010;194(4):933–7.
7. von Ballmoos MW, Haring B, Juillerat P, Alkadhi H. Meta-analysis: diagnostic performance of low-radiation-dose coronary computed tomography angiography. Ann Intern Med. 2011;154(6):413–20.
8. Menke J, Unterberg-Buchwald C, Staab W, Sohns JM, Seif Amir Hosseini A, Schwarz A. Head-to-head comparison of prospectively

triggered vs retrospectively gated coronary computed tomography angiography: meta-analysis of diagnostic accuracy, image quality, and radiation dose. Am Heart J. 2013;165(2):154–63. e3.
9. Meyer M, Haubenreisser H, Schoepf UJ, Vliegenthart R, Leidecker C, Allmendinger T, et al. Closing in on the K edge: coronary CT angiography at 100, 80, and 70 kV-initial comparison of a second- versus a third-generation dual-source CT system. Radiology. 2014;273(2):373–82.
10. Gordic S, Desbiolles L, Sedlmair M, Manka R, Plass A, Schmidt B, et al. Optimizing radiation dose by using advanced modelled iterative reconstruction in high-pitch coronary CT angiography. Eur Radiol. 2016;26(2):459–68.
11. Leschka S, Stolzmann P, Schmid FT, Scheffel H, Stinn B, Marincek B, et al. Low kilovoltage cardiac dual-source CT: attenuation, noise, and radiation dose. Eur Radiol. 2008;18(9):1809–17.
12. Hausleiter J, Martinoff S, Hadamitzky M, Martuscelli E, Pschierer I, Feuchtner GM, et al. Image quality and radiation exposure with a low tube voltage protocol for coronary CT angiography results of the PROTECTION II Trial. JACC Cardiovasc Imaging. 2010;3(11):1113–23.
13. Hausleiter J, Meyer T, Hadamitzky M, Huber E, Zankl M, Martinoff S, et al. Radiation dose estimates from cardiac multislice computed tomography in daily practice: impact of different scanning protocols on effective dose estimates. Circulation. 2006;113(10):1305–10.
14. Park YJ, Kim YJ, Lee JW, Kim HY, Hong YJ, Lee HJ, et al. Automatic Tube Potential Selection with Tube Current Modulation (APSCM) in coronary CT angiography: comparison of image quality and radiation dose with conventional body mass index-based protocol. J Cardiovasc Comput Tomogr. 2012;6(3):184–90.
15. Naoum C, Blanke P, Leipsic J. Iterative reconstruction in cardiac CT. J Cardiovasc Comput Tomogr. 2015;9(4):255–63.
16. Hell MM, Bittner D, Schuhbaeck A, Muschiol G, Brand M, Lell M, et al. Prospectively ECG-triggered high-pitch coronary angiography with third-generation dual-source CT at 70 kVp tube voltage: feasibility, image quality, radiation dose, and effect of iterative reconstruction. J Cardiovasc Comput Tomogr. 2014;8(6):418–25.
17. Leschka S, Kim CH, Baumueller S, Stolzmann P, Scheffel H, Marincek B, et al. Scan length adjustment of CT coronary angiography using the calcium scoring scan: effect on radiation dose. AJR Am J Roentgenol. 2010;194(3):W272–7.
18. Hausleiter J, Meyer T, Hermann F, Hadamitzky M, Krebs M, Gerber TC, et al. Estimated radiation dose associated with cardiac CT angiography. JAMA. 2009;301(5):500–7.